Supporting Information

Where is the nano? Analytical approaches for the detection and quantification of TiO$_2$ engineered nanoparticles in surface waters

Andreas Gondikas[§,¤], Frank von der Kammer[§], Ralf Kaegi[#], Olga Borovinskaya[¶], Elisabeth Neubauer[§], Jana Navratilova[§,‡], Antonia Praetorius[§,$], Geert Cornelis[‖], Thilo Hofmann[§]

[§]Department of Environmental Geosciences and Environmental Science Research Network, University of Vienna, Vienna 1090, Austria

[¤] Current address: Department of Marine Sciences, Kristineberg, Fiskebäckskil 45178, Sweden

[#]Department of Process Engineering, Eawag, Duebendorf 8600, Switzerland

[¶]TOFWERK, 3600 Thun, Switzerland

[‡]Current address: National Exposure Research Lab, United States Environmental Protection Agency, Research Triangle Park, NC 27709, U.S.A.

[$]Research Platform Nano-Norms-Nature, University of Vienna, Vienna, Austria

[‖]Department of Soil and Environment, Swedish University of Agricultural Sciences, 75651 Uppsala, Sweden

Table S1: Theoretical detection limit of anthropogenic Ti in sediments and SPM using bulk concentrations and bulk elemental ratios. The calculation is based on the assumption that the anthropogenic input needs to be higher than the natural variation, here defined as three times the standard deviation of concentrations in the sediments of the reference lake (N=3) and the SPM of the Old Danube lake during the non-bathing months (N=16). Concentrations of Al in the sediments and the SPM were 18,300 ± 5,800 ppm and 24,200 ± 7,600 ppm, respectively; concentrations of V in the sediments and SPM were 27.7 ± 5.6 ppm and 93.4 ± 34.6 ppm, respectively.

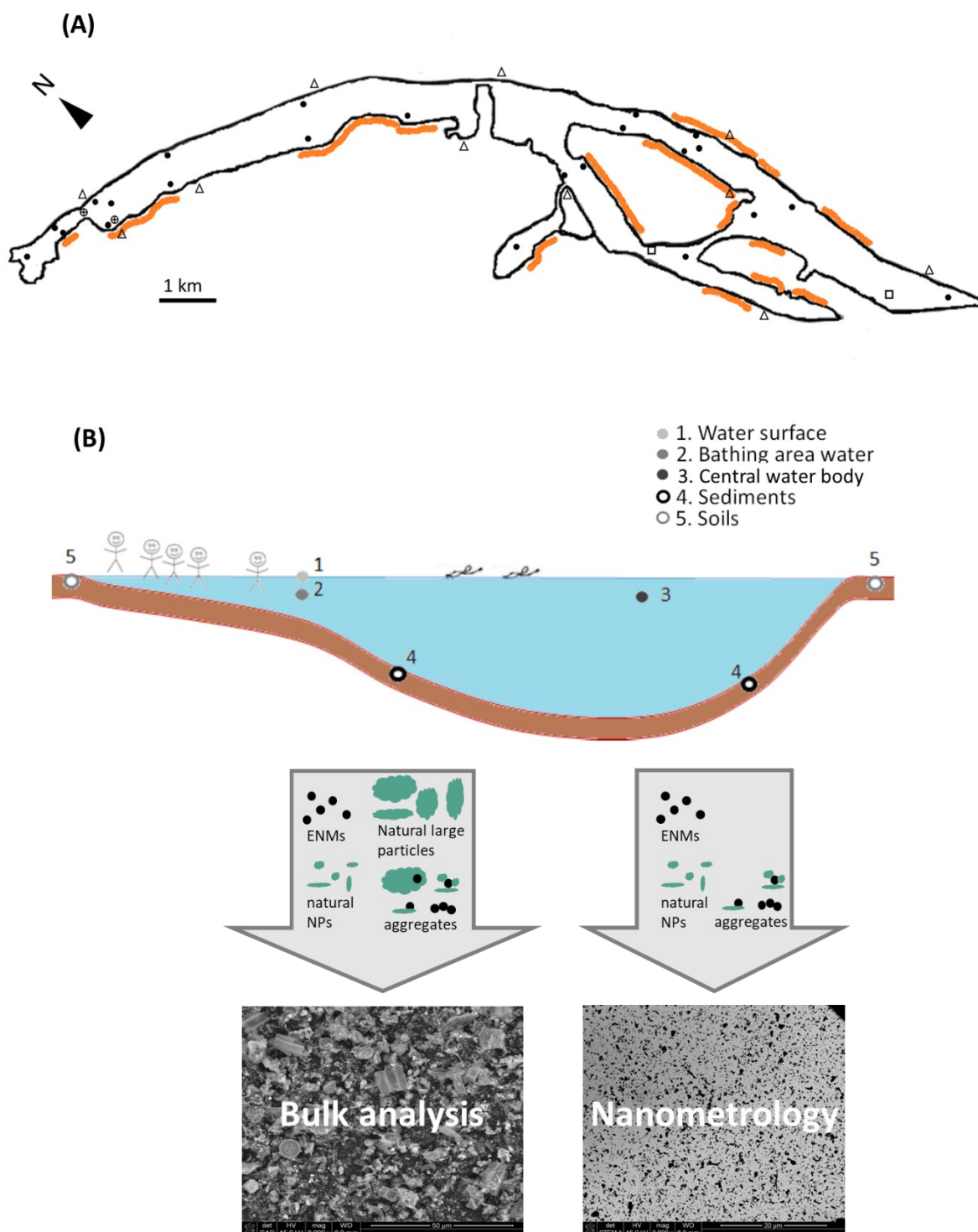|	Monitoring parameter	Average	Standard deviation (σ)	Detectable anthropogenic Ti input (>3*σ)
Sediments	mg-Ti/ kg-sediment	1,160	370	1,110 (mg-Ti/ kg-sediment)
	mg-Ti/ mg-Al	0.0642	0.0105	577 (mg-Ti/ kg-sediment)
	mg-Ti/ mg-V	41.4	7.1	590 (mg-Ti/ kg-sediment)
SPM	mg-Ti/ kg-SPM	964	332	996 (mg-Ti/ kg-SPM)
	mg-Ti/ mg-Al	0.0405	0.0086	624 (mg-Ti/ kg-SPM)
	mg-Ti/ mg-V	11.0	3.4	953 (mg-Ti/ kg-SPM)

Figure S1. (A) Schematic of the Old Danube lake. Sediment sampling locations are marked with solid circles, water sampling locations with encircled crosses, sediment core samples with empty squares, and topsoil samples with empty triangles. The approximate locations of areas that are used as bathing beaches are marked in orange. (B) Schematic showing the five types of samples: water samples from

the bathing area, the air-water interface (surface water), and the central water body of the lake, and

samples of lake sediment and adjacent topsoil. Typical SEM images of samples are shown to

demonstrate the differences in sample handling for the two analytical approaches: bulk analysis and
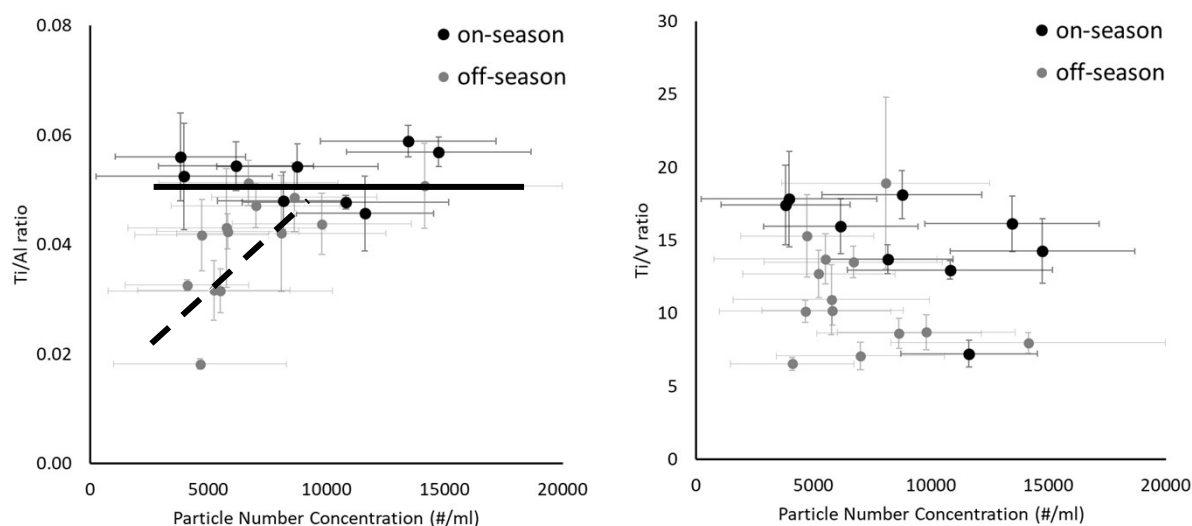
nanometrology.

Figure S2. Bulk SPM elemental ratios Ti/Al (left) and Ti/V (right) plotted against particle number concentrations (determined with spICPMS) for samples collected before and after the bathing season (off-season) and samples collected during the bathing season (on-season). Error bars of particle numbers indicate the standard deviation of three replicate samples; error bars of SPM elemental ratios indicate the standard deviation of up to three replicate filters. The solid line (on-season) and broken line (off-season) only serve as an eye-guide to visualize the general trends.
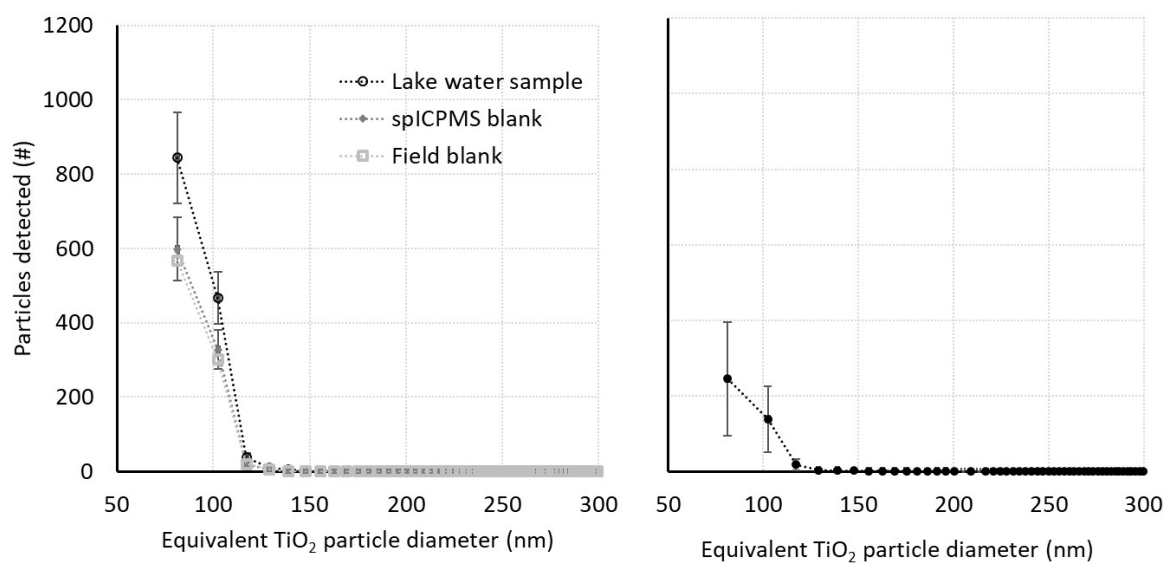
Figure S3. Left: Typical size-based frequency plots of a lake water sample from the central water body, a fieldblank sample, and an instrument blank sample (spICPMS blank). Error bars represent the standard deviation of three replicate samples for the lake water and the field blank sample and 15 replicate samples for the spICPMS blank samples. Intensities have been converted to equivalent TiO_2 particle diameter on the x-axis. Right: Plot of size-based number distribution with blank values subtracted against equivalent TiO_2 particle diameters. Error bars represent the standard deviation calculated from error propagation.
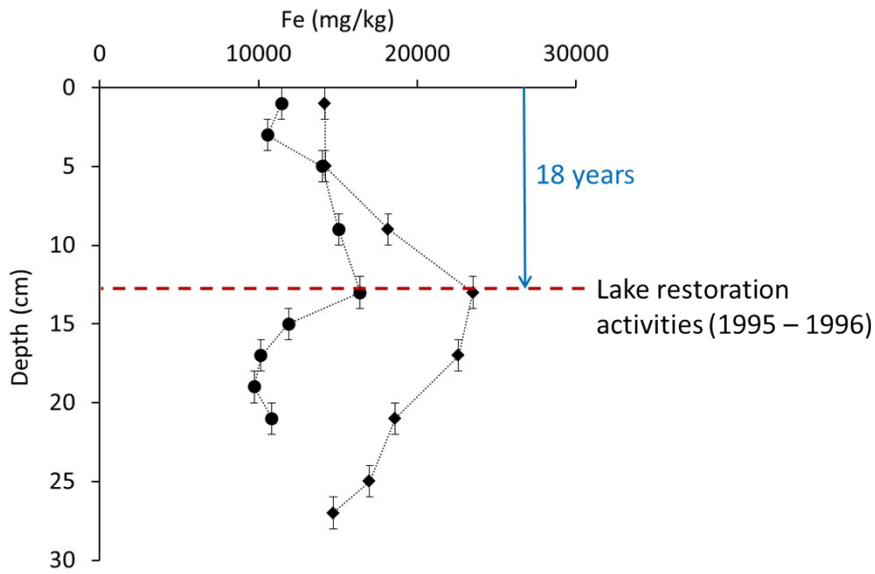
Figure S4. Iron concentration as a function of depth in sediment core samples collected from the Old Danube lake. The two datasets represent iron concentrations from two separate core samples. Maximum iron concentrations are expected at depths that correspond to restoration activities in 1995 – 1996, and are marked with a red dashed line. This data was used to calculate an average sediment accumulation rate.
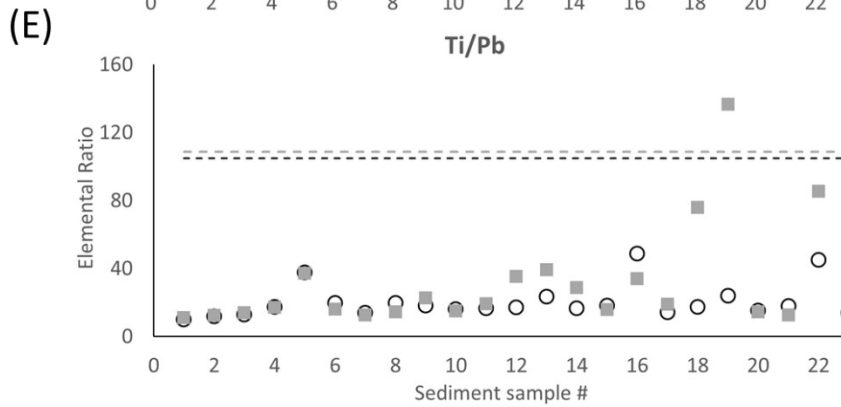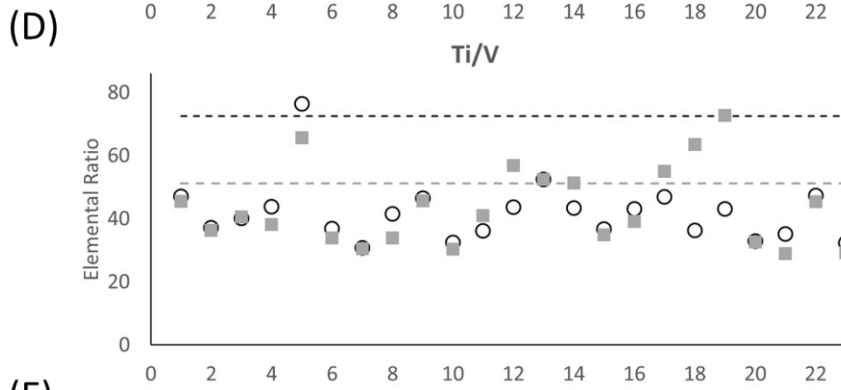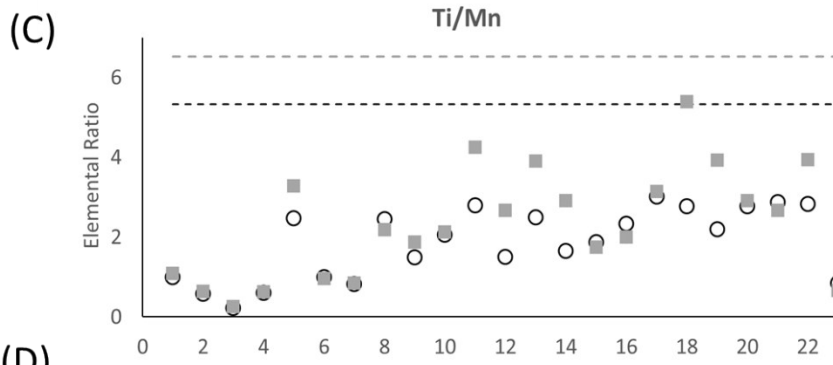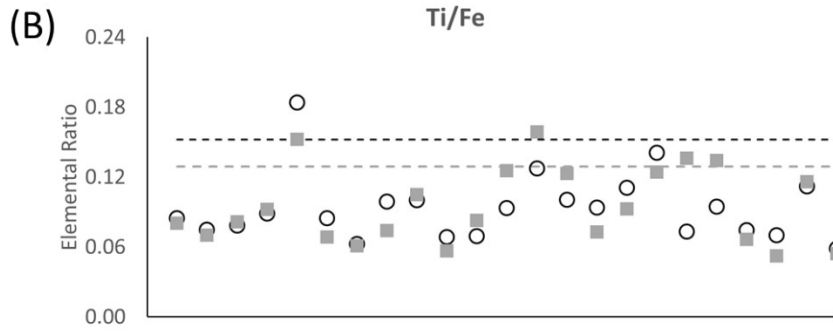
(A) Ti/Al

(B) Ti/Fe

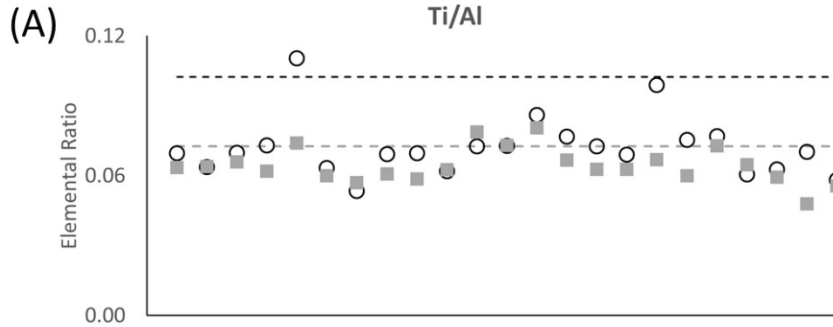(C) Ti/Mn

(D) Ti/V

(E) Ti/Pb

Figure S5. Elemental ratios of Ti to Al (A), Fe (B), Mn (C), V (D), and Pb (E) in sediments collected from 23 locations throughout the Old Danube lake. Data are shown for two sediment size fractions: < 63 μm (empty circles) and 63 – 250 μm (solid squares). Natural variation was determined from sediments in the reference lake: the average ratio plus 3 times the standard deviation is shown for the < 63 μm (black dashed line) and 63 – 250 μm (grey dashed line) fractions.
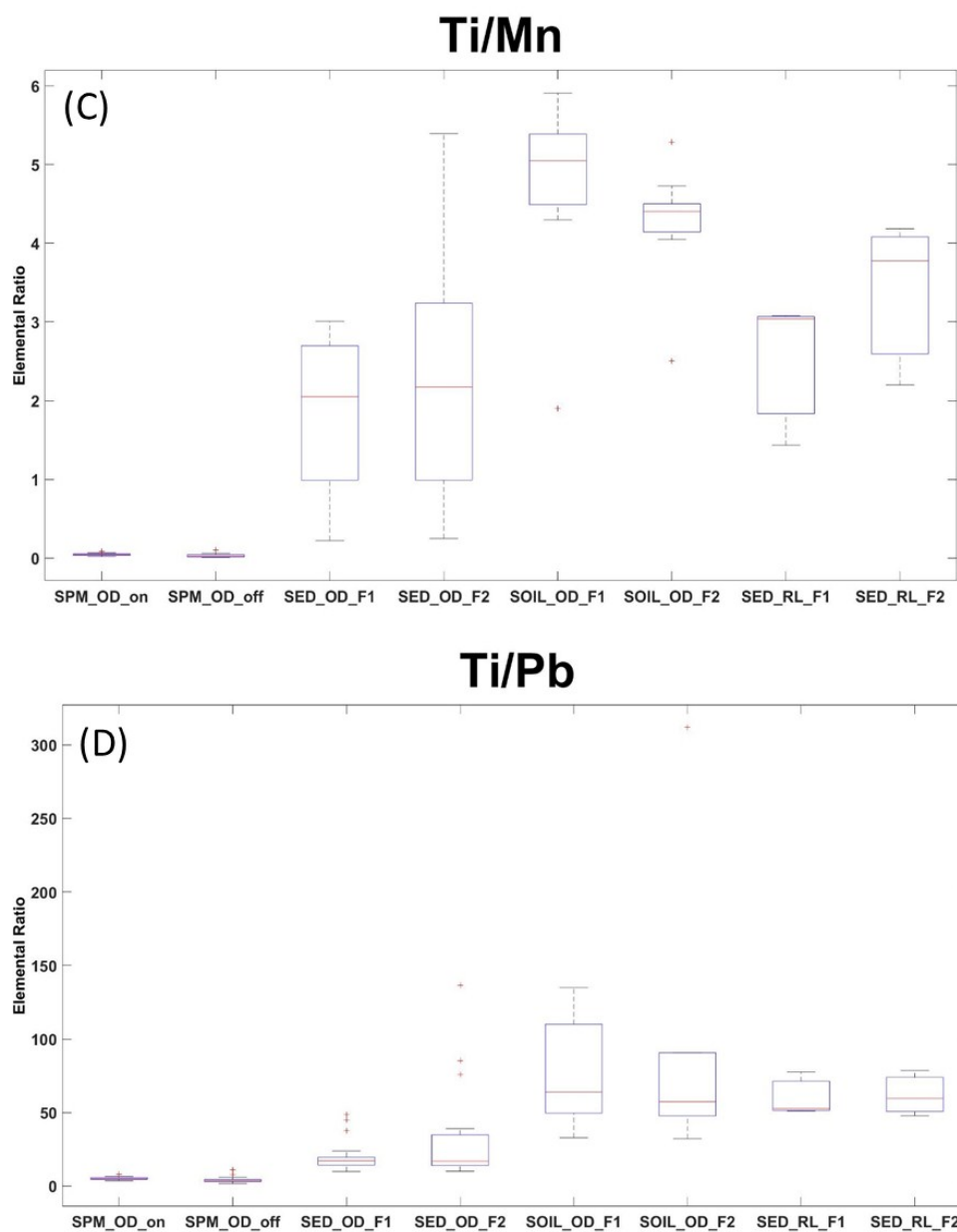
Ti/Al

(A)

Ti/Fe

(B)
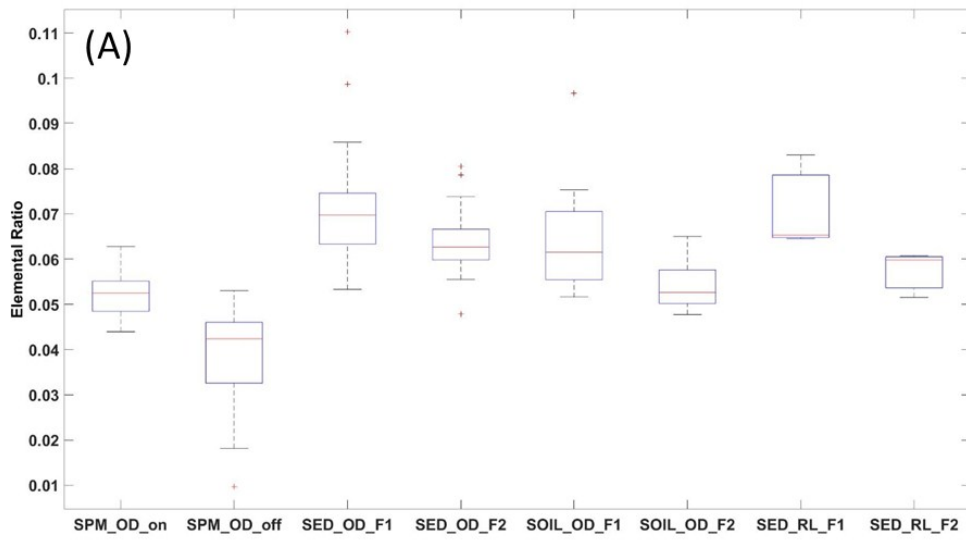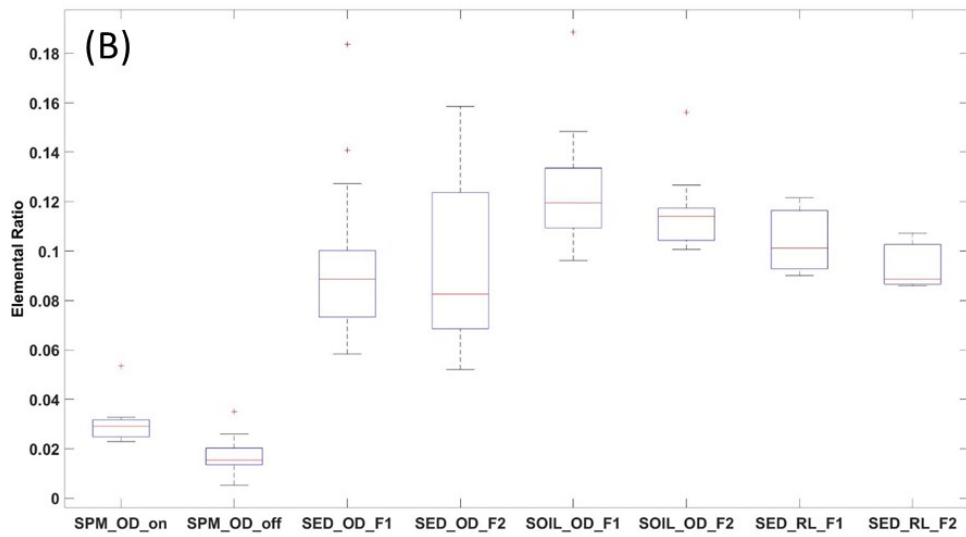
Figure S6. Boxplots of elemental ratios of titanium to aluminum (A), iron (B), manganese (C), and lead (D) in SPM, sediments (SED), and topsoil (SOIL) samples from the Old Danube lake (OD) and the reference lake (RL). Sediment and topsoil samples were split into two fractions: < 63 μm (F1) and 63 – 250 μm (F2).

Alternative methods for sampling the air-water-interface (AWI)

AWI samples were collected in July and August using two different methods:

Method 1 involved placing nylon nets with mesh sizes 20 μm and 100 μm, on the water's surface and then carefully removing them. The nylon nets were stored in 50 mL centrifuge tubes for transport and centrifuged upon arrival at the laboratory (1200 g, 20 minutes). Blank samples were prepared by wetting nylon nets with ultrapure water and subjecting them to the same procedure as the samples.

Method 2 involved submerging a glass plate (30 cm by 40 cm) vertically in the lake water. On extraction the water film on the glass plate was transferred to a sampling vessel with the help of a rubber window wiper. The glass plate was then re-submerged and the procedure repeated until a volume of 100 mL was obtained. Blanks were produced by wetting the glass plate with ultrapure water and collecting the water with the rubber window wiper. Results are plotted in Figure S7. Unfiltered total samples and (ultrapure water) field blanks are also shown for comparison. The nylon net blank samples yielded measureable concentrations of Ti and the Ti concentrations in the AWI samples collected by nylon net did not differ significantly from those in the blank sample. The glass plate samples yielded higher Ti concentrations than the unfiltered samples and the field blank samples, and on three sampling dates they were also significantly higher than the blank sample, ranging from 6.5 to 25 μg/L.
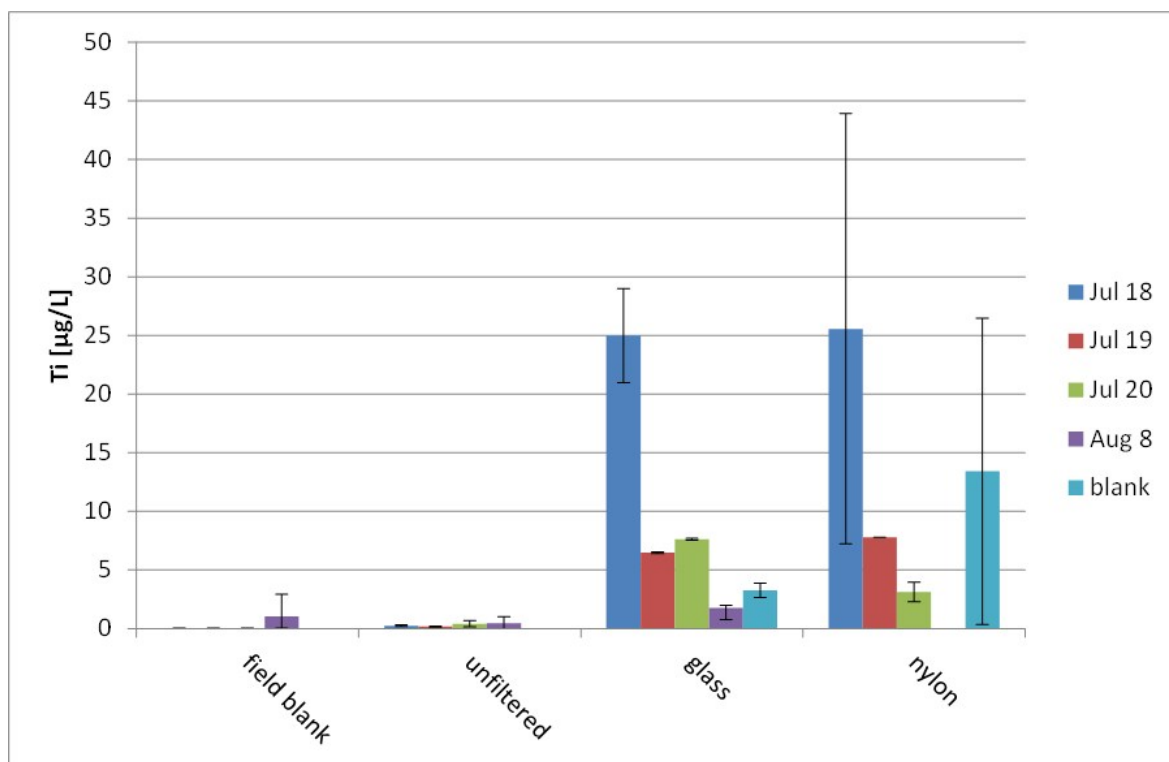
Figure S7. Titanium concentrations in AWI samples collected with a glass plate and with a nylon net.